Vol. 2, No. 3, 2012, 9–17

Shahrood University of Technology

Journal of Solid and Fluid Mechanics

One-Dimensional design of a three-stage axial compressor with Its 3D numerical simulation

M. Behnia [1] and M. Nili-Ahmadabadi [2,*]

[1] MSc., Dept. of Mechanical Engineering, Isfahan University of Technology, Isfahan, Iran
[2] Assistant Prof., Dept. of Mechanical Engineering, Isfahan University of Technology, Isfahan, Iran

Abstract

In this research, one-dimensional design of a three-stage axial compressor is performed to reach an adequate pressure ratio and efficiency in design point conditions with rotational speed of 38000 rpm and mass flow rate of 3.2kg/s. At first, some constraints such as Dehaller number more than 0.7 for all sections of rotor and stator, and relative Mach number less than 0.8 at rotor blade tip are considered. In this design, hub diameter is equal to shaft diameter in each stage. In order to reduce rotor blade tip diameter or tip Mach number at the first stage, some inlet guide vanes are utilized. Therefore, the rotor and stator blades can be designed based on reaction coefficient of 0.5. The output of the one-dimensional design program is calculation of all geometric parameters such as blades inlet and outlet angles, blades length and diameter, solidity coefficient, number of blades and blades stagger angles at three different sections of hub, mid and tip in compliance with the constraints. Thus, 3D shape of the blades can be generated. To ensure the performance characteristic of the designed compressor at design and off design conditions, the 3D designed geometry is modeled in BLADE GEN software and then is transferred to TURBO GRID for grid generation. Finally, 3D numerical solution of fluid flow through all blades passages is solved by CFX flow solver. In this approach, compressible flow equations are solved according to the pressure based method with SST turbulence model. The numerical solution results indicate that the designed compressor has a maximum pressure ratio of 1.8 with efficiency of 80% which is acceptable for a primary design.

Keywords: Axial compressor; One dimensional design; Numerical simulation; Dehaller.

1. Introduction

Compressor is one of the most important components of gas turbine engines. Complex flow and high velocity, as well as high blade loading, affect its effective performance. In 1853, basic operations of a multi-stage axial compressor were characterized [2, 3] and since then compressor work was widely studied. Complex mechanism of a compressor has caused its design to be very competitive. In the late 1940s and early 1950s, turbines and axial compressors were designed based on experimental data. Howell [4] designed an axial compressor on the mid-section based on the wind tunnel test data. Moreover, some information about profile losses and secondary losses was obtained from the wind tunnel test data.

One-dimensional models are extensively used for design and performance analysis of compressors. Greitzer [5, 6] invented a lumped-volume method to investigate the surge and separation based on fixed properties of the compressor. Morini [7] developed a one-dimensional non-linear dynamic model to investigate the transient behavior in compression systems. Furthermore, two and three-dimensional models were presented to describe the separation initiation and system performance in existence of separation.

To simulate the separation inception in an axial compressor, Takata and Nagato [8] developed a two-dimensional model assuming that the blade row is replaced by a semi-driving disc.

Tauveron [9] developed new empirical equations to evaluate compressor performance in all flow regions and used them for dynamic simulations.

* Corresponding author, Phone: +983113915240
Email: m.nili@cc.iut.ac.ir

Shao et al. [10] investigated the effect of blade load distribution and blade tip clearance on leakage losses using Denton model.

2. One-Dimensional Design

In this part, the steps used in one-dimensional design procedure are described.

1. In all stages, blade hub diameter of the rotor and stator is considered equal to the motor shaft diameter obtained from maximum allowable stress in shaft (d_h=0.1127m).

2. Since the aim of this study is to obtain the minimum engine diameter while relative Mach number of the rotor blade tip retains less than 0.8 to prevent local shocks, the first stage rotor blade tip diameter is obtained in a way that the tip relative Mach number becomes equal to 0.8. The calculation of the first stage rotor blade tip diameter is done through an iterative process.

3. Using the engine inlet conditions including the atmospheric static pressure and the rest static temperature, the inlet Mach number and axial flow velocity are obtained from mass flow equation at the engine inlet.

$$\dot{m} = \rho_1 A_1 C_{m1} = \pi(r_{1s}^2 - r_{1h}^2)\rho_1 C_{m1} \quad (1)$$

4. In all stages, axial velocity is constant and equal to the inlet axial velocity (C_m=const).

5. In this study, a three-stage axial compressor is designed to reach an identical pressure ratio with acceptable efficiency. Since each stage has its own least Dehaller number according to reference [1]. The maximum diffusion coefficient for rotor and stator is equivalent to Dehaller number of 0.7. The critical rotor and stator section for satisfying the Dehaller number of 0.7 is the hub and tip section, respectively.

$$Dehaller = \frac{C_1}{C_2} = \frac{W_2}{W_1} \quad (2)$$

On the other hand, in a multi-stage axial compressor with equal pressure ratio in each stage, the Dehaller number decreases toward the final stages. As a result, the last stage is the most critical one in which the Dehaller number should be equal to 0.7.

6. Since the inlet flow is axial, if IGV is not used, the flow enters directly into the rotor and so the rotor blade tip relative Mach number will be higher than that with IGV. In other words, if IGV is used, the rotor blade tip diameter or relative Mach number of rotor blade tip will decrease for a specific mass flow rate. Furthermore, the reaction coefficient can be considered equal to 0.5. Thus, we consider IGV in our design procedure.

7. In axial compressors, the maximum efficiency is obtained when the reaction coefficient is equal to 0.5 [1].

$$R_n = 1 - \frac{C_{u1} + C_{u2}}{2u} \quad (3)$$

8. Considering the reaction coefficient to be equal to 0.5 for all sections from hub to tip, the velocity triangles of the first stage are obtained in a way that the Dehaller number equals 0.74. This value makes the last stage hub Dehaller number equal to 0.7. Thus, the stage pressure ratio is obtained using the Euler equation.

$$\Delta_1^2 h_0 = \Delta_1^2 (u C_u) \quad (4)$$

9. Having the inlet and outlet flow angles in all sections, the adequate blade profile is selected from NACA-Mellor diagrams. Fig. 2 shows an example of NACA-Mellor diagrams. However, the IGV blades are designed based on double circular arc profiles.

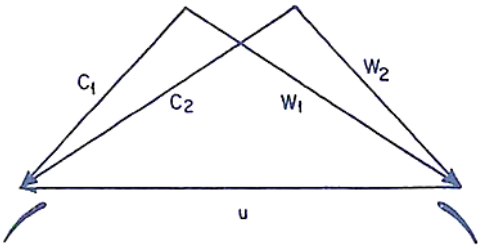

Fig. 1. Reactive compressor velocity triangle

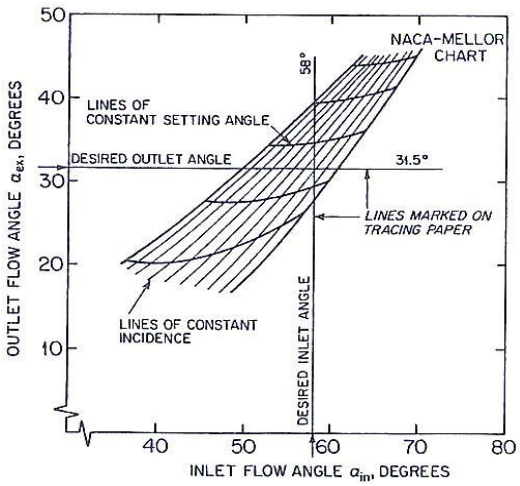

Fig. 2. NACA-Mellor diagram [1]

As obvious in Fig. 2, in addition to the blade profile selection, it is possible to select adequate stagger angle and solidity coefficient. These parameters are used to determine the number of blades in each stage. The number of guide vanes is modified based on a trial and error by numerical simulation whose results will be presented at the next section. Finally, the compressor length is obtained 0.18m. The results of the one-dimensional design are tabulated in Tables 1-4.

Table 1. Inlet guide vane

Parameter \ Part	hub	mead	tip
α_1 (◦)	0	0	0
α_2 (◦)	28	53	69
λ(◦)	14	27	35
σ	2.88	2.52	2.34
Z		33	

Table 2. First stage

d_{t1} (m)		0.1807	
d_{t2} (m)		0.17333	
Pr		1.29	
Z		16r-25s	
Parameter \ Part	hub	mead	tip
α_1 (◦)	45	50	53
α_2 (◦)	18	31	41
Airfoil type	65(18)	65(18)	65(18)
λ(◦)	30	36	45
σ	1	0.5	0.5
M_{rel1}	0.7026	0.7475	0.806
ψ	-0.512	-0.302	-0.2
ϕ	0.7475	0.5743	0.4662
Dh	0.74	0.7741	0.808

Table 3. Second stage

d_{t1} (m)		0.17333	
d_{t2} (m)		0.1643	
Pr		1.29	
Z		22r-27s	
Parameter \ Part	hub	mead	tip
α_1 (◦)	46	48	52
α_2 (◦)	16.5	29	38
Airfoil type	65(18)	65(18)	65(18)
λ(◦)	28	37	43
σ	1.25	1.25	0.5
M_{rel1}	0.6852	0.725	0.78
ψ	-0.555	-0.345	-0.235
ϕ	0.7475	0.59	0.486
Dh	0.723	0.754	0.787

Table 4. Third stage

d_{t1} (m)		0.1643	
d_{t2} (m)		0.156	
Pr		1.29	
Z		25r -27 s	
Parameter \ Part	hub	mead	tip
α_1 (◦)	46	49	51
α_2 (◦)	15	26	35
Airfoil type	65(18)	65(18)	65(18)
λ(◦)	26	35	39
σ	1.25	0.75	0.75
M_{rel1}	0.6662	0.7	0.736
ψ	0.6043	-0.4	-0.2843
ϕ	0.7475	0.61	0.5128
Dh	0.705	0.73	0.761

3. Numerical simulation

Having obtained the required parameters from one-dimensional design program, appropriate profiles in all three sections of hub, mid and tip are selected using NACA-Mellor diagrams. Then, the three-dimensional shape of the blades can be drawn in BLADE GEN software. It is noticeable that the chord length is constant from hub to tip for IGV and stator blades, while it is changed from hub to tip for rotor blades which causes the solidity coefficient to be changed and a trapezoid shape to be obtained. Furthermore, because the compressor is reactive, the stator and rotor blade profiles are analogous at all stages while their concavities are reversed. Fig. 3 shows a 3D view of the first-stage designed rotor blade.

Fig. 3. 3D Designed rotor blade

The most important step of the numerical simulation of flow inside the turbomachines is the grid generation. Selection of grid type and locations for grid refinements are additional important duties. In this simulation, TURBO GRID software is used for grid generation. Hexahedra elements are used for grid generation of all stages. The finer grids were used for zones having high gradients such as near-wall region. The errors in the solution related to the grid must become extinct for increasing mesh accuracy. The compressor pressure ratio and efficiency at flow conditions with rotational speed 38000 rpm and mass flow rate 3.2kg/s was taken as the parameters to evaluate three grid configurations (Table 5) and to determine the influence of grid size on the solution. In Table 5, it is observed how the calculated compressor pressure ratio and efficiency reach an asymptotic value as the number of elements increases. According to this Table, the grid with one million elements was considered to be sufficiently reliable to ensure mesh independency as shown in Fig. 4. In the generated grid,

the Y+ value on the walls is less than 20. Verification of CFX flow solver has been done for another compressor in Ref [11]. In that reference, the comparison between CFX results and experimental results shows that the uncertainty of total pressure ratio is equal to 0.9%.

Table 5. Effect of grid size on pressure ratio and efficiency of the compressor

Number of elements	*Pr*	η (%)	Error (%)
650000	1.83	81.6	2.2-2.5
1000000	1.8	80	0.56-0.5
1700000	1.79	79.6	-

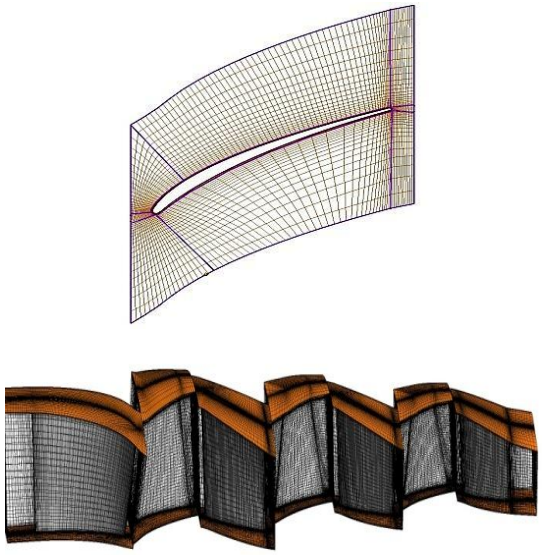

Fig. 4. Generated grid for rotor and stator blades

Finally, flow inside the compressor is simulated using CFX flow solver to evaluate the designed compressor and to validate one-dimensional design method. In CFX flow solver, compressible flow equations with pressure based method and SST turbulence model are solved. Table 6 shows the governing equations and boundary conditions. Meanwhile, the outlet pressure is obtained from one-dimensional design program.

The results of the numerical simulation are shown in Figs. 5–8. As shown in Fig. 5, the Mach number reaches to1 near the leading edge. Also, it is higher at the tip section which makes it more critical. The local oblique shock near the leading edge at tip section causes the local separation to occur on the suction surface. Fig. 6 show that the streamlines at hub and tip section. As shown in this figure, except the stator tip section at the last stage, the streamlines are attached to the blades in other regions. Moreover, it is noticeable that streamlines at hub section are more smoothed than tip section. In Fig. 7, a contour plot for relative stagnation pressure in the rotor and absolute stagnation pressure in the stator is shown at all stages. At the rotor blade tip and the stator blade hub, the stagnation pressure losses can be observed which is consistent with Fig. 5 and Fig. 6. According to Figure 8, the pressure ratio of the simulated compressor is more than 1.8. Fig. 9 indicates that the flow at the compressor outlet is approximately uniform. It shows that there are two low momentum regions near the hub and shroud in the side of suction surface.

Table 6. Governing equations and boundary conditions

governing equations	Continuity equation	
	Momentum equation	
	Energy equation	
	Turbulence equation	
boundary conditions	T_{01}(K)	300
	P_2(Pa)	217344
	m (kg/s)	3.2
	Periodicity method	Rotational
	Interface type	Mixing plane
	Turbulence model	SST

It should be noted that the number of inlet guide vanes are modified by several numerical simulations.

Figure 10 shows stream lines at the first-stage rotor tip section for two designs with different numbers of guide vanes. As shown, increasing the number of inlet guide vanes causes the separation on the rotor blades to be removed. Indeed, excessive increase of IGV blades number causes the friction losses to be increased.

Pressure ratio at each stage and total efficiency from numerical simulation is tabulated in Table 7.

Table 7. Pressure ratio and total efficiency at different stages

First stage	1.2
Second stage	1.24
Third stage	1.21
Total efficiency(%)	80

In Fig. 11, compressor total pressure ratio obtained from numerical simulation is drawn versus mass flow rate at different constant rotational speed. It shows that the total pressure ratio reduces with increasing mass flow rate and decreasing rotational speed except for the surge region. Compressor total pressure ratio is defined as the following relation:

$$Pr = \frac{P_{02}}{P_{01}} \quad (5)$$

It should be noted that surge phenomenon occurs in rotating speed of 25000rpm and 38000rpm at mass flow rate 2.5kg/s and 3.2 kg/s, respectively.

In Fig. 12, compressor total to total isentropic efficiency obtained from numerical simulation is

shown versus mass flow rate at different constant rotational speed. The total to total efficiency is defined as the following relation:

$$\eta = \frac{T_{01}\left(Pr^{(\gamma-1)/\gamma} - 1\right)}{T_{02} - T_{01}} \tag{6}$$

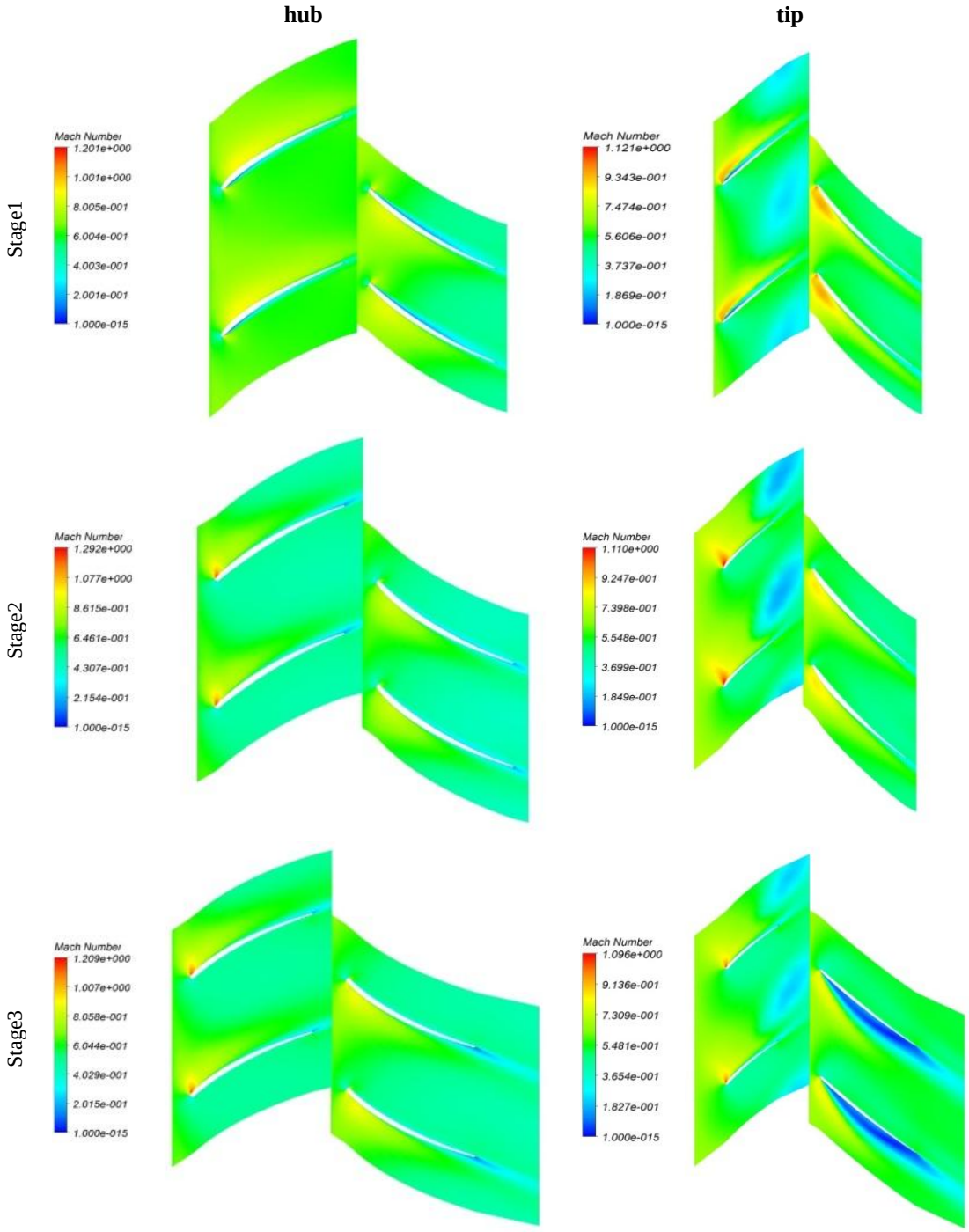

Fig. 5. Mach number contour at hub and tip section.

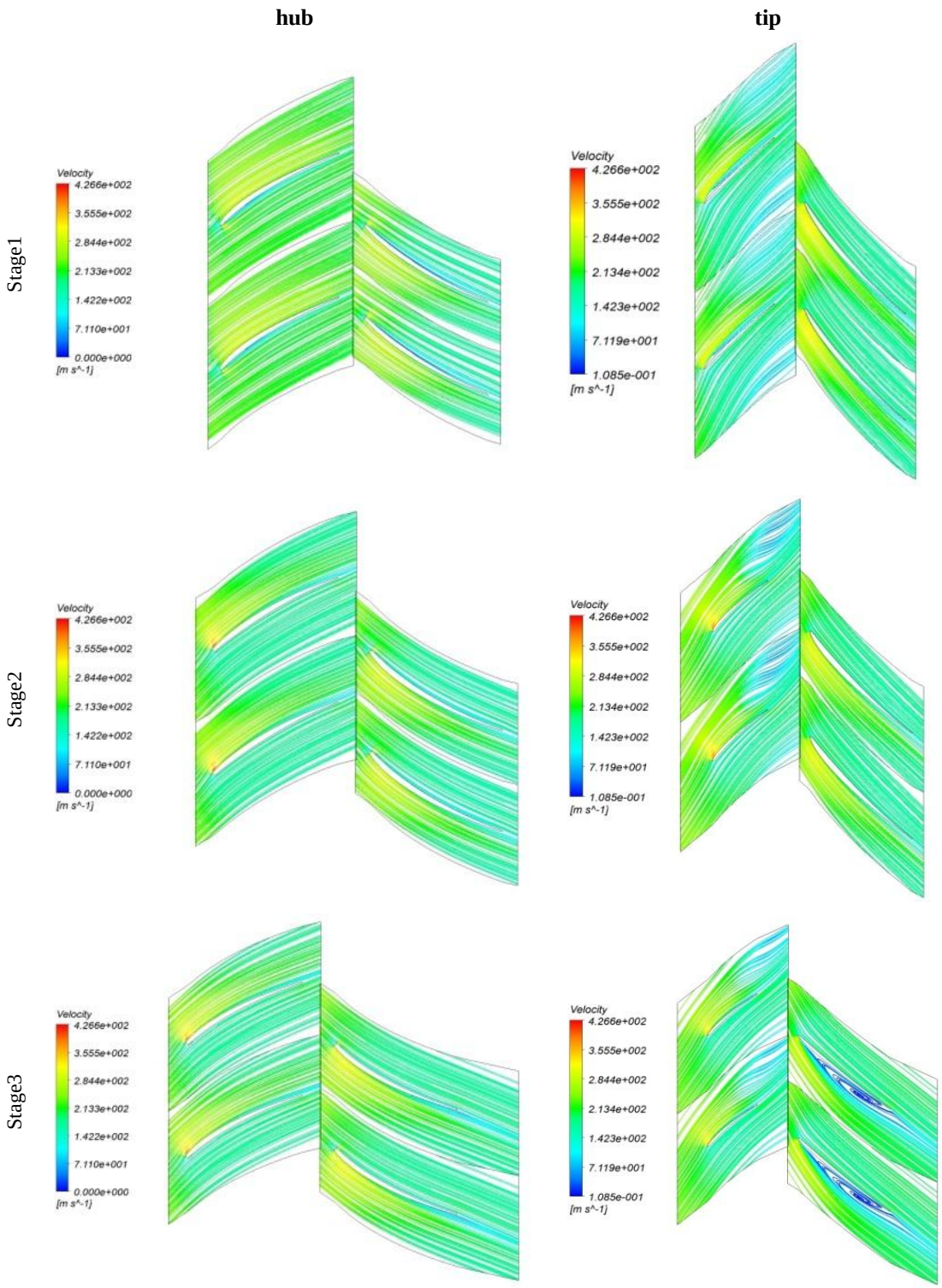

Fig. 6. Streamline at hub and tip section.

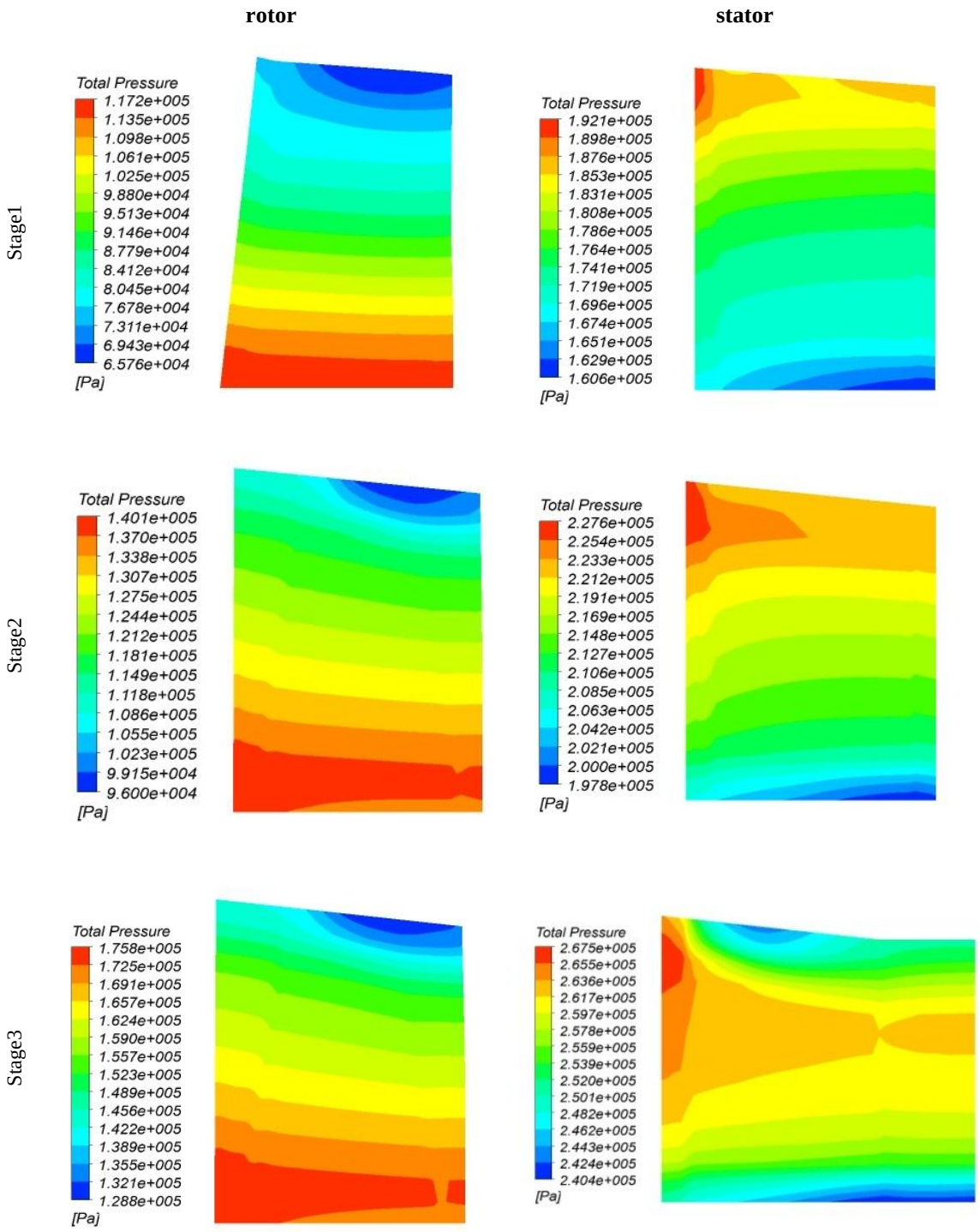

Fig. 7. Change of relative stagnation pressure from hub to tip.

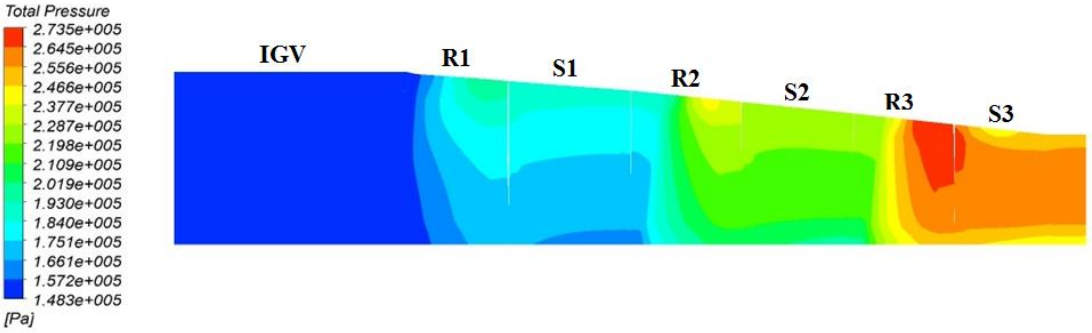

Fig. 8. Increase Stagnation pressure inside of the compressor

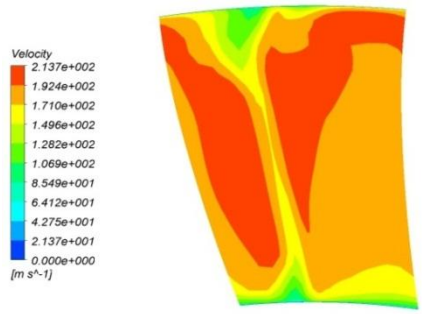

Fig. 9. Velocity contour at the compressor outlet

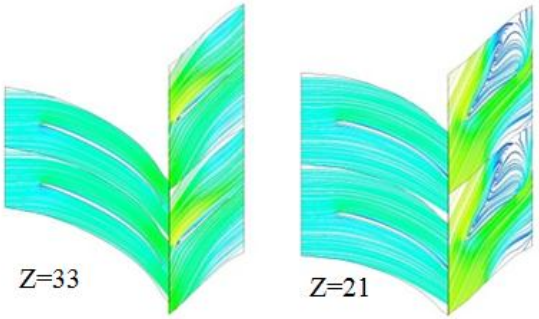

Fig. 10. Stream lines at tip section for two designs with different numbers of inlet guide vanes

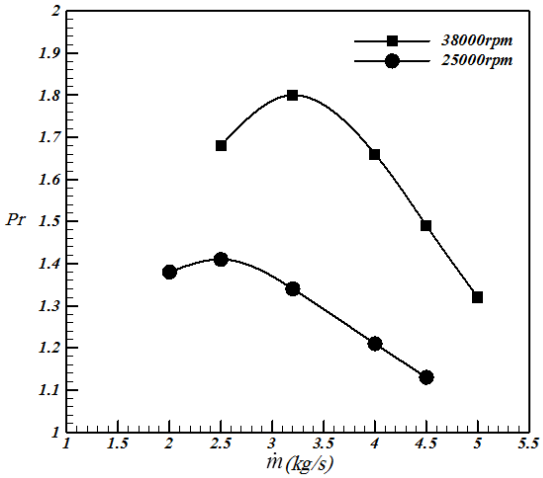

Fig. 11. Numerical compressor total pressure ratio versus mass flow rate at different constant rotational speed

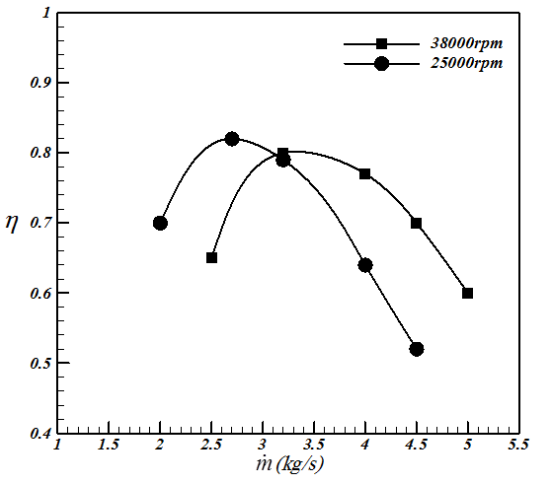

Fig. 12. Numerical compressor isentropic efficiency versus mass flow rate at different constant rotational speed

4. Conclusion

In this study, a three-stage axial compressor with identical pressure ratio was designed by one-dimensional design method in which Dehaller and Mach number constraints were satisfied. This design was done in design point conditions with rotational speed of 38000 rpm and mass flow rate of 3.2kg/s. Calculation of all geometric parameters including the blades inlet and outlet angles, blades length and diameter, solidity coefficient, number of blades and stagger angle of the blade in all sections were done. To investigate the results obtained from the one-dimensional design, the full 3D numerical analysis inside the compressor was accomplished. 3D numerical results indicated that the one-dimensional design is suitable as a design method for preliminary design of compressor. Numerical results showed the total pressure ratio and total to total efficiency of the compressor is 1.8 and 0.8, respectively. The differences between one-dimensional design and numerical simulation are due to three-dimensional flows inside the compressor, shock waves, secondary flows and etc. which were not considered in one-dimensional design.

Nomenclature

A	Area
C	Absolute velocity
d	diameter
Dh	Dehaller number
h	enthalpy
M	Mach number
$\dot{m}$	Mass Flow Rate
P	Pressure
Pr	Total to Total Pressure Ratio
r	Rotor
s	Stator
T	Temperature
W	Relative velocity
Z	Number of Blades
α	Blade Angle
ρ	Density
γ	Specific Heat Ratio
η	Total-to-total Isentropic Efficiency
ω	Compressor Rotational Speed
σ	Solidity coefficient
λ	stagger Angle
ψ	Loading coefficient
ϕ	Flow coefficient

Subscripts

h	Hub
rel	Relative
t	Tip
0	stagnation
1	Inlet
2	Outlet

References

[1] Wilson DG, Korakianitis Th (1998) The design of high-efficiency turbomachinery and gas turbines. MIT Press. 349–354.

[2] Horlock JH (1985) Axial flow compressors. Butterworths Scientific Publications, London.

[3] Gostelow JP (1984) Cascade Aerodynamics, Pergamon Press, New York, NY.

[4] Howell AR (1942) The present basis of axial flow compressor design: Part 1- cascade theory and performance. Aeronautical Research Council R and M. No. 2095.

[5] Greitzer EM (1978) Surge and rotating stall in axial flow compressors. Part I: Theoretical compression system model. Journal of Engineering for Power 100: 190–198.

[6] Greitzer EM (1978) Surge and rotating stall in axial flow compressors. Part II: Experimental results and comparison with theory. Journal of Engineering for Power 100: 199–217.

[7] Morini M (2007) Development of a one-dimensional modular dynamic model for simulation of surge in compression systems. Journal of Turbomachinery 129: 437–447

[8] Takata H, Nagato S (1972) Nonlinear analysis of rotating stall. Journal of Engineering for Power 94: 279–293.

[9] Tauveron N, Saez M, Ferrand P, Leboeuf F (2007) Axial turbomachine modeling with a 1D axisymmetric approach. application to gas cooled nuclear reactor. Nuclear Engineering and Design 237: 1679–1692

[10] Shao W, Ji L (2007) Basic analysis of the tip leakage mixing loss. ASME paper GT2007–27616.

[11] Nili-Ahmadabadi M, Durali M, Hajilouy A (2010) A novel quasi-3d design method for centrifugal compressor meridional plane. ASME paper GT2010–23341.